11th World Congress on Computational Mechanics (WCCM XI)
5th European Conference on Computational Mechanics (ECCM V)
6th European Conference on Computational Fluid Dynamics (ECFD VI)
E. Oñate, J. Oliver and A. Huerta (Eds)

# STRUCTURAL DEFECTS AND DYNAMIC PROPERTIES OF METALS

**ALEXANDER E. MAYER[*], ELIJAH N. BORODIN[†] AND POLINA N. MAYER[*]**

[*] Chelyabinsk State University (CSU), Department of Physics
Bratyev Kashirinykh 129, 454001 Chelyabinsk, Russia
e-mail: mayer.al.evg@gmail.com, polina.nik@mail.ru

[†] Institute of Problems of Mechanical Engineering RAS (IPME RAS)
V.O. Bolshoj pr. 61, 199178 St. Petersburg, Russia
email: elbor7@gmail.com

**Key Words:** *Dislocations, Twins, Grain Boundaries, Plasticity, Dynamical Problems.*

**Abstract.** A computational plasticity model with accounting of coupled evolution of the dislocations, twins and grain boundaries in metals under the dynamic loading is presented. The model is based on our previous results for the dislocation plasticity and the grain boundary sliding, but generalizes them and accounts twins in addition. It includes equations of the mechanics of continua for elastic-plastic medium, where the plastic deformation tensor is determined as a result of the structural defects evolution in the material. The model is self-consistent and allows determining of mechanical properties in wide range of strain rates and thermodynamic conditions as well as modification of the defect subsystems. The equations and parameters, its numerical implementation and some of obtained results are presented.

## 1 INTRODUCTION

Constitutive equations are necessary for numerical simulation of materials behaviour in the framework of continuum mechanics. Shear stresses in metals are determined by elastic-plastic properties and plasticity model is a substantial part of the constitutive equations. Experimentally obtainable rates of deformation vary from almost zero–at quasi-static deformation–up to $10^9$ $s^{-1}$–at the thin foils irradiation by the ultra-short laser pulses [1,2]. Therefore, the plasticity model is greeted to be a wide-range one, which means that it should be valid in a vide range of strain rates as well as in a wide range of thermodynamic parameters. Accounting of structural defects (dislocations, grain boundaries, micro-twins) as physical carriers of plasticity is a natural way to construct such a wide-range plasticity model.

Here we present our plasticity model based on the structural defects evolution. Next processes are accounted: motion, generation and immobilization of dislocations [3,4], formation, growth and immobilization of twins [5], the grain boundary sliding [6,7]. Interaction of deferent defect subsystems is accounted through their barrier stresses.

Evolution of defect subsystems is described through equations for their concentration (or density) and other characteristics (velocity of dislocations, radius and thickness of twins, for example). It allows to calculate the plastic strain tensor and the shear stresses–through the

generalized Hook's law. Calculation of the structural defects evolution is performed in each physically small volume of metal simultaneously with calculation of its dynamic deformation on the basis of the continuum mechanics equations. Mechanical response of substance is calculated in this way as well as the defect subsystems modification [8].

## 2 MATHEMATICAL MODEL–CONTINUUM MECHANICS

Total plastic strain of polycrystalline metal can be represented as a result of the combined action of three competing processes: i) the dislocation motion, ii) the mechanical twining and iii) sliding along the grain boundaries. According to this viewpoint, the plastic deformation tensor $w_{ik}$ is represented by the next sum of three tensors: $w_{ik} = w_{ik}^{\mathrm{D}} + w_{ik}^{\mathrm{tw}} + w_{ik}^{\mathrm{gb}}$, where $w_{ik}^{\mathrm{D}}$ is the part of plastic deformation caused by the dislocation motion, $w_{ik}^{\mathrm{tw}}$ is caused by the mechanical twinning and $w_{ik}^{\mathrm{gb}}$ is caused by the grain boundary sliding. Determination of these tensors through evolution of defect subsystems will be considered in the following section.

The common part of the mathematical model consists of three conservation laws. The first one of them is the continuity equation:

$$\frac{1}{\rho}\frac{d\rho}{dt} = -\sum_{k=1}^{N}\frac{\partial \upsilon_k}{\partial x_k}, \tag{1}$$

where $\rho$ is the substance density; $\upsilon_k$ is velocity vector; $x_k$ is the Cartesian coordinates; $N$ is the number of dimensions of the considered problem, index $k$ numerates space directions. The total time derivatives are used in Eq. (1) and following equations, which are valid for Lagrangian particles moving with substance. The equation of substance motion:

$$\rho\frac{d\upsilon_i}{dt} = -\frac{\partial P}{\partial x_i} + \sum_{k=1}^{N}\frac{\partial S_{ik}}{\partial x_k}, \quad i = 1,\ldots,N, \tag{2}$$

where $P$ is the pressure or spherical part of stresses, which is determined from a wide-range equation of state $P = P(\rho, U)$ [9,10]; $S_{ik}$ is the tensor of stress deviators, which characterizes the shear stresses; $U$ is the part of internal energy, connected with the spherical part of stresses, its value is determined from the energy conservation law in the next form:

$$\rho\frac{dU}{dt} = \frac{P}{\rho}\frac{d\rho}{dt} + \sum_{i=1}^{N}\sum_{k=1}^{N} S_{ik}\frac{dw_{ik}}{dt}, \tag{3}$$

where the second term in the right-hand part is the heat release due to the plastic strain.

The generalized Hooke law [11] with accounting of the plastic strain $w_{ik}$ is used for determination of the stress deviators:

$$S_{ik} = 2G\left[u_{ik} - \frac{1}{3}\delta_{ik}\sum_{l=1}^{N}u_{ll} - w_{ik}\right], \quad i = 1,\ldots,N, \quad k = 1,\ldots,N, \tag{4}$$

where $G = G(T, P)$ is the shear modulus, which depends on temperature and pressure [12]; $\delta_{ik}$ is the bivalent mixed tensor; $u_{ik}$ is the geometrical deformation, induced by the

macroscopic motion of substance, which is determined by the next equation:

$$\frac{du_{ik}}{dt} = \frac{1}{2}\left[\frac{\partial v_i}{\partial x_k} + \frac{\partial v_k}{\partial x_i}\right] + \frac{1}{2}\sum_{l=1}^{N}\left\{u_{il}\left(\frac{\partial v_k}{\partial x_l} - \frac{\partial v_l}{\partial x_k}\right) + u_{lk}\left(\frac{\partial v_i}{\partial x_l} - \frac{\partial v_l}{\partial x_i}\right)\right\}, \tag{5}$$

where the first term in the right-hand part is the infinitesimal strain rate tensor; the second term accounts for the change of the geometrical deformation tensor components in the laboratory coordinate system due to the substance rotation [13], which is essential for two- or three-dimensional cases.

## 3 MATHEMATICAL MODEL–EVOLUTION OF STRUCTURAL DEFECTS

Three main types of structural defects–dislocations, micro-twins and grain boundaries–are considered here together with their contributions in the total plastic strain. The particular case of monocrystal corresponds to zero contribution of the grain boundaries $w_{ik}^{\mathrm{gb}} = 0$. Contribution of twining can be zero as well $w_{ik}^{\mathrm{tw}} = 0$ for metals with the suppressed twining, aluminum for example. All three parts are accounted in the common case.

Submodels of the dislocation plasticity and the mechanical twining consist of kinetics equations for defects ensembles and equations for corresponding contributions, $w_{ik}^{\mathrm{D}}$ and $w_{ik}^{\mathrm{tw}}$, in the total plastic strain. Dislocations are characterized by scalar densities of mobile and immobilized dislocations and velocity of mobile dislocations; these quantities are determined for each possible slip system of dislocations in the considered metal and for each physically small volume of substance. Thus we use the continuous theory of dislocations. Twins are supposed to be cylindrical and characterized by concentrations of mobile and immobilized twins (with fixed boundaries), their radius and thickness. All possible crystallographic orientations of twins are also accounted. Submodel of the grain boundary sliding is more simple, it includes only equation for corresponding contribution $w_{ik}^{\mathrm{gb}}$, while the boundaries state and the grain size are supposed to be unchangeable.

### 3.1 Dislocations

The plastic deformation tensor of the dislocation plasticity $w_{ik}^{\mathrm{D}}$ can be found from the generalized Orowan equation [14]:

$$\frac{dw_{ik}^{\mathrm{D}}}{dt} = \sum_{\beta}\frac{1}{2}\left(b_i^{\beta} n_k^{\beta} + b_k^{\beta} n_i^{\beta}\right) V_{\mathrm{D}}^{\beta} \rho_{\mathrm{D}}^{\beta} + \frac{1}{2}\sum_{l=1}^{N}\left\{w_{il}^{\mathrm{D}}\left(\frac{\partial v_k}{\partial x_l} - \frac{\partial v_l}{\partial x_k}\right) + w_{lk}^{\mathrm{D}}\left(\frac{\partial v_i}{\partial x_l} - \frac{\partial v_l}{\partial x_i}\right)\right\}, \tag{6}$$

where the first term in the right-hand part is the plastic strain rate itself while the second term accounts rotation of the substance elements, like in Eq.(5). Index $\beta$ numerates the slip systems of dislocations in the material, which is characterized by the Burgers vector $b_i^{\beta}$ and by the normal $n_i^{\beta}$ to the slip plane; $\rho_{\mathrm{D}}^{\beta}$ is the dislocation density of mobile dislocations in the corresponding slip system; $V_{\mathrm{D}}^{\beta}$ is velocity of these dislocations relative to the substance.

One has to take into account the different crystallographic orientations of lattice in different grains for description of the polycrystalline metals. Simulations [3] had shown that

the most suitable oriented slip planes are activated first of all. Therefore, it is enough to account only such "active" planes, which orientations are close throughout the sample, regardless of the grain boundaries. This is very handy approximation, especially for the nanocristalline metals, where the grains are much smaller than the numerical grid resolution.

The core of the dislocation plasticity model [3,4] consists of the motion and kinetics equations. The equation of dislocations motion is the next:

$$m_0 \xi_\beta^3 \frac{\mathrm{d}V_\mathrm{D}^\beta}{\mathrm{d}t} = \left[ \sum_{i=1}^{N} \sum_{k=1}^{N} S_{ik} b_i^\beta n_k^\beta \pm \frac{1}{2} bY \right] - B \xi_\beta^3 V_\mathrm{D}^\beta , \tag{7}$$

where $\xi_\beta = 1/\sqrt{1-\left(V_D^\beta / c_\mathrm{t}\right)^2}$ is a quasi-relativistic factor [15], which reflects the restriction that $\left|V_D^\beta\right| < c_\mathrm{t}$; $c_\mathrm{t} = \sqrt{G/\rho}$ is the transverse sound speed of the material; $m_0 \approx 10^{-16}$ kg/m is the rest mass of dislocations; $Y$ is the static yield strength; $B$ is the phonon drag coefficient, it describes the viscous resistance to the dislocation motion [16]. Dislocations move only if the force of the shear stresses (the first term in the square brackets in Eq.(7)) is higher than the resistance of the Peierls relief, inclusions and other defects, which is $bY/2$; the sign "$\pm$" means that the resistance is always directed opposite to the dislocation motion.

The kinetics equations for mobile $\rho_\mathrm{D}^\beta$ and immobilized $\rho_\mathrm{I}^\beta$ dislocations [4]:

$$\frac{\mathrm{d}\rho_\mathrm{D}^\beta}{\mathrm{d}t} = Q_\mathrm{D}^\beta - Q_\mathrm{I}^\beta - Q_\mathrm{Da}^\beta , \qquad \frac{\mathrm{d}\rho_\mathrm{I}^\beta}{\mathrm{d}t} = Q_\mathrm{I}^\beta - Q_\mathrm{Ia}^\beta , \tag{8}$$

where $Q_\mathrm{D}^\beta$ is the generation rate of the mobile dislocations; $Q_\mathrm{I}^\beta$ is the rate of immobilization; $Q_\mathrm{Da}^\beta$ and $Q_\mathrm{Ia}^\beta$ are the annihilation rates of mobile and immobilized dislocations correspondently:

$$Q_\mathrm{a}^\beta = k_\mathrm{a} b \left|V_\mathrm{D}^\beta\right| \rho_\mathrm{D}^\beta \left(2\rho_\mathrm{D}^\beta + \rho_\mathrm{I}^\beta\right) - \left|V_\mathrm{D}^\beta\right| \rho_\mathrm{D}^\beta / d , \qquad Q_\mathrm{Ia}^\beta = k_\mathrm{a} b \left|V_\mathrm{D}^\beta\right| \rho_\mathrm{D}^\beta \rho_\mathrm{I}^\beta , \tag{9}$$

where $k_a$ is the annihilation factor; $d$ is the grain diameter in polycrystals; $b$ is the modulus of Burgers vector of dislocations. Rates of generation and immobilization are the next:

$$Q_\mathrm{D}^\beta = \frac{0.1}{\varepsilon_\mathrm{D}} \left\{ 2B \cdot c_\mathrm{t}^2 \cdot \left[ \xi_\beta - 1 \right] + b \cdot Y \cdot \left|V_\mathrm{D}^\beta\right| \right\} \cdot \rho_\mathrm{D}^\beta , \tag{10}$$

$$Q_\mathrm{I}^\beta = V_\mathrm{I} \left(\rho_\mathrm{D}^\beta - \rho_0\right) \sqrt{\rho_\mathrm{I}^\beta} , \tag{11}$$

where $\varepsilon_\mathrm{D} \approx 8\,\mathrm{eV}/b$ is the energy of the dislocations formation per unit length. The multiplier in curly brackets in Eq. (10) is the energy dissipation rate per unit length of dislocation–it is the sum of work against the phonon friction and the work against the resistance force [15]. Eq. (11) describes the immobilization process, where parameter $\rho_0 \approx 10^7$ cm$^{-2}$ is the minimal dislocations density, which is necessary for their consolidation in the structures [4]. This expression is written from the assumption that all excess mobile dislocations will be immobilized in structures with the characteristic time $\tau_{I\beta} \approx r_{I\beta}/V_\mathrm{I}$, where $r_{I\beta} \approx (\rho_I^\beta)^{-1/2}$ is the average distance between the immobile dislocations. Parameter $V_\mathrm{I}$ means a characteristic velocity of the

dislocations movement during the process of consolidation; it is determined by internal stresses.

The drag coefficient $B$ depends on the temperature [17]:

$$B = T \cdot \left(4\theta^2 k_{\mathrm{B}}^3\right) / \left(h^2 c_{\mathrm{b}}^3\right), \tag{12}$$

where $k_B$ is the Boltzmann constant; $h$ is the Planck constant; $\theta$ is the parameter with the dimensionality of temperature. The static yield strength is determined by the following relation:

$$Y = Y_0 + AGb\sqrt{\rho_{\mathrm{I}}} + k_{\mathrm{HP}} / \sqrt{d} + k_{\mathrm{TW}} / \sqrt{\Delta}\ , \tag{13}$$

where $\rho_{\mathrm{I}}$ is the total scalar density of immobilized dislocations (the sum over all slip planes); $\Delta$ is an average distance between the twins; $A$ is the interaction constant of dislocations, $k_{\mathrm{HP}}$ is the Hall-Petch constant and $k_{\mathrm{TW}}$ is similar constant for twins. In the right-hand part of Eq.(13): $Y_0$ is the resistance of Peierls relief and point defects (inclusions); the second term is resistance of immobile dislocations (the Taylor law), the third term is contribution of grain boundaries (the Hall-Petch law) and the last term expresses the resistance of twins in a similar way to the grain boundaries [5].

Parameters of the dislocation plasticity model have been found in [4] by comparison with velocity histories of back surface at plate impact tests; they are presented in Tabel 1.

**Table 1**: Parameters of the plasticity model

| Metal | Al | Cu | Ni |
|---|---|---|---|
| $Y_0$, MPa | 22 | 30 | 40 |
| $\theta$, K | 430 | 280 | 300 |
| $A$ | 6 | 4 | 0.3 |
| $V_{\mathrm{I}}$, m/s | 5 | 2 | 1 |
| $\nu$ | 0.357 | 0.337 | 0.3 |

### 3.2 Twins

Twining becomes an alternative plasticity mechanism at low temperatures and high strain rates [18,19]. The stacking fault energy $\gamma_{\mathrm{SF}}$ is the main parameter determining the material tendency to undergo the twining. Metals with low stacking fault energy (less than 0.1 J/m$^2$), for example various steels, copper, silver, nickel and their alloys, are disposed to twinning.

Plastic deformation caused by twinning can be expressed through its volume fraction:

$$\frac{dw_{ik}^{\mathrm{TW}}}{dt} = \sum_{\gamma} \frac{d\alpha^{\gamma}}{dt}\left(\tau_i^{\gamma} n_k^{\gamma} + \tau_k^{\gamma} n_i^{\gamma}\right)\varepsilon_{\mathrm{TW}} + \frac{1}{2}\sum_{l=1}^{N}\left\{ w_{il}^{\mathrm{TW}}\left(\frac{\partial \upsilon_k}{\partial x_l} - \frac{\partial \upsilon_l}{\partial x_k}\right) + w_{lk}^{\mathrm{TW}}\left(\frac{\partial \upsilon_i}{\partial x_l} - \frac{\partial \upsilon_l}{\partial x_i}\right)\right\}, \tag{14}$$

where $\alpha^{\gamma}$ is the volume fraction of twinned material; $\varepsilon_{\mathrm{TW}}$ is the deformation of twinned material with respect to initial one, for example $\varepsilon_{\mathrm{TW}} = 1/\sqrt{2}$ in fcc metals [19]; unit vectors $\tau_k^{\gamma}$ and $n_k^{\gamma}$ describes crystallographic orientation of twins; index $\gamma$ numerates all possible

orientations. The second term in the right-hand part plays the same role as in Eqs. (5) and (6).

We suppose that twins are cylindrical and have the same radius and thickness in a physically small substance element, than the volume fraction is equal to

$$\alpha^{\gamma} = N_{\mathrm{TW}}^{\gamma} \cdot \left(2\pi R_{\mathrm{TW}}^{\gamma} \cdot h_{\mathrm{TW}}^{\gamma}\right) + N_{\mathrm{IM}}^{\gamma} \cdot \left(2\pi R_{\mathrm{IM}}^{\gamma} \cdot h_{\mathrm{IM}}^{\gamma}\right), \tag{15}$$

where $N_{\mathrm{TW}}^{\gamma}$ and $N_{\mathrm{IM}}^{\gamma}$ are the local concentrations of twins, mobile and immobilized correspondently; $R_{\mathrm{TW}}^{\gamma}$ and $R_{\mathrm{IM}}^{\gamma}$ are radiuses of mobile and immobilized twins; $h_{\mathrm{TW}}^{\gamma}$ and $h_{\mathrm{IM}}^{\gamma}$ are their thicknesses. All these values are determined by the kinetics of twins.

Energy of a twin consists of the surface part determined by the stacking fault energy, the energy in external stresses and the energy of elastic deformations of the surrounding matrix [20]. Differentiation of this energy over radius or thickness gives the forces tending to change the corresponding size of the twin:

$$F_R^{\gamma} = 4\pi\varepsilon_{\mathrm{TW}} \cdot R_{\mathrm{TW}}^{\gamma} h_{\mathrm{TW}}^{\gamma} \cdot \sum_{k=1}^{N}\sum_{i=1}^{N} S_{ik} n_i^{\gamma} \tau_k^{\gamma} - 2\pi\gamma_{\mathrm{SF}} \cdot \left(2R_{\mathrm{TW}}^{\gamma} + h_{\mathrm{TW}}^{\gamma}\right) - \Phi \cdot \left(h_{\mathrm{TW}}^{\gamma}\right)^2, \tag{16}$$

$$F_h^{\gamma} = 2\pi\varepsilon_{\mathrm{TW}} \cdot \left(R_{\mathrm{TW}}^{\gamma}\right)^2 \cdot \sum_{k=1}^{N}\sum_{i=1}^{N} S_{ik} n_i^{\gamma} \tau_k^{\gamma} - 2\pi\gamma_{\mathrm{SF}} \cdot R_{\mathrm{TW}}^{\gamma} - 2\Phi \cdot R_{\mathrm{TW}}^{\gamma} h_{\mathrm{TW}}^{\gamma}, \tag{17}$$

where $\Phi = 2\pi^3\left(2-\nu\right)/\left[3\left(1-\nu\right)\right]G\varepsilon_{\mathrm{TW}}^2$, $\nu$ is the Poisson ratio (see Table 1). Growth of twin radius or thickness is connected with motion of twinning dislocations at its edges, which are the partial dislocations. The balance between the described above forces (expressions (16) and (17)) and the drag force acting on these dislocations allows one to find the growth equations:

$$\frac{dR_{\mathrm{TW}}^{\gamma}}{dt} = F_R^{\gamma} / B', \quad \frac{dh_{\mathrm{TW}}^{\gamma}}{dt} = F_h^{\gamma} / B', \tag{18}$$

where $B' \approx B/3$ is the drag coefficient of partial dislocations.

Expressions (16) and (17) give the critical radius $R_{\mathrm{cr}}^{\gamma}$ and the thickness $h_{\mathrm{cr}}^{\gamma}$ of twin at which forces are equal to zero–a twin larger than the critical one will grow up. Immobilized twins can not grow in radius but they can change its thickness similar to Eqs. (17), (18).

The last part of the twinning model is the kinetics equations for concentrations of twins. We have written them from energetic consideration supposing that the twinning becomes an active channel of plastic strain then the dislocation plasticity becomes ineffective. Twins are experimentally observed usually then the dislocation plasticity is suppressed. Effectiveness of the dislocation channel is restricted by annihilation of dislocations (see Eq. (9)). A part of plastically dissipated energy spends on formation of new defects [21,22], but in conditions of active annihilation this energy can not be stored in the dislocation subsystem and should be stored in other types of defects, twins for example. Thus, the generation rate of twins

$$\dot{N}_{\mathrm{TW}}^{\gamma+} = \varepsilon_{\mathrm{D}}\left(Q_{\mathrm{Da}}^{\beta} + Q_{\mathrm{Ia}}^{\beta}\right) / \left(4\pi\left(R_{\mathrm{cr}}^{\gamma}\right)^2 \gamma_{\mathrm{SF}} \cdot \gamma_0\right), \tag{19}$$

where $Q_a = \sum_{\beta} Q_{\mathrm{Da}}^{\beta} + Q_{\mathrm{Ia}}^{\beta}$ is the total annihilation rate of dislocations; $\gamma_0$ is the total number of possible orientations of twins. A twin becomes immobilized then it reaches a grain

boundary or another twin; the immobilization rate can be written as follows:

$$\dot{N}_{\mathrm{TW}}^{\gamma-} = N_{\mathrm{TW}}^{\gamma} \cdot \left| dR_{\mathrm{TW}}^{\gamma} / dt \right| \cdot \left( \Delta^{-1} + d^{-1} \right). \tag{20}$$

The average distance between the twins $\Delta$ is connected with their volume fraction [18] $\Delta^{-1} = \sum_{\gamma} \left[ \alpha^{\gamma} / \left\{ \left(1-\alpha^{\gamma}\right) h_{\mathrm{TW}}^{\gamma} \right\} \right]$. Finally the required kinetics equations are the next:

$$\frac{dN_{\mathrm{TW}}^{\gamma}}{dt} = \dot{N}_{\mathrm{TW}}^{\gamma+} - \dot{N}_{\mathrm{TW}}^{\gamma-}, \qquad \frac{dN_{\mathrm{I}}^{\gamma}}{dt} = \dot{N}_{\mathrm{TW}}^{\gamma-}. \tag{21}$$

Implementation of this twinning model to the plate impact tests gives results corresponding to the experimental observations as it had been shown in [5].

### 3.3 Grain boundary sliding

Here we define the plastic strain $w_{ik}^{\mathrm{gb}}$ caused by the grain boundary sliding. We consider a shift of a grains layer relative to another layer. Such shifts should take place along the directions of maximal shear stress first of all. Index $\alpha$ numerates all possible planes of grains shifting; $n_i^{\alpha}$ is the unit normal to one of these planes. The force per unit square applied to the corresponding plane is equal to $\sigma_{ik} n_k^{\alpha}$, and the force component, which acts in the tangent direction $\tau_i$ to the plane, is equal to the convolution product $\sigma_{ik} n_k^{\alpha} \tau_i = S_{ik} n_k^{\alpha} \tau_i$. We denote $\tau_i^{\alpha}$ as the direction of the tangent vector corresponding to the maximum shear stresses (tangential force) applied to the plane. Then the maximal shear stress acting on the layer of grains can be represented as $\sigma_{\tau}^{\alpha} = S_{ik} n_i^{\alpha} \tau_k^{\alpha}$.

The shift of grain layer on one grain diameter demands for each grain in the sliding plane to deform two grains in the neighbor plains. It leads to appearance of a barrier resistance stress $y_b$ which depends on the grain size [6]. It is the stress which the external shear stresses must exceed for initiating of the grain boundary sliding. Viscous force appears in the grain boundaries due to diffusion, which counteracts the sliding of grain layers; it can be characterized by the relaxation time $\mathrm{T}$. As a result, the next equation can be written for the plastic deformation caused by the grain boundary sliding [6,7]:

$$\frac{dw_{ik}^{\mathrm{gb}}}{dt} = \sum_{\alpha} \tau_i^{\alpha} n_k^{\alpha} \frac{\sigma_{\tau}^{\alpha} - y_b}{2G\mathrm{T}} + \frac{1}{2} \sum_{l=1}^{N} \left\{ w_{il}^{\mathrm{gb}} \left( \frac{\partial \upsilon_k}{\partial x_l} - \frac{\partial \upsilon_l}{\partial x_k} \right) + w_{lk}^{\mathrm{gb}} \left( \frac{\partial \upsilon_i}{\partial x_l} - \frac{\partial \upsilon_l}{\partial x_i} \right) \right\}. \tag{22}$$

This approach is similar to the Maxwell model for a highly viscous liquid [11] with an exception of the barrier resistance stress $y_b$.

Using a linear approximation, one can obtain the following expression for the relaxation time of the grain boundary sliding [6] from data of the molecular dynamics simulation [23]:

$$\mathrm{T} = d \frac{k_B T}{12 G b \nu_D V_s} \exp\left( \frac{U_s}{k_B T} \right), \tag{23}$$

where $\nu_D$ is the Debye frequency; $V_s \sim b^3$ is the activation volume; $U_s$ is the activation

energy–of the order of activation energy of viscous flow in the melt [24].

The next expression for the threshold stress $y_b$ had been obtained in [6]

$$y_b = 0.01\frac{G}{1-\nu}\left(1-\frac{\delta}{d}\right)^2, \tag{24}$$

where the grain boundary thickness $\delta$ is about 1 nanometer.

## 4 NUMERICAL IMPLEMENTATION

The described above plasticity model is numerically realized in CRS computer program in 1D and 2D cases. This program is designed to simulate various intensive actions on metal: high-speed impact, intensive electron, ion and laser irradiation.

Method of separation by physical processes is used with the next subproblems: i) substance dynamics (Eqs. (1)-(3)); ii) dislocations kinetics and motion; iii) twinning; iv) grain boundary sliding. Equations for all these processes are solved independently on each time step, and the data exchange takes place at the end of each step. Subproblem of the substance dynamics are solved by modification of the numerical method [25]. Modification consists in eliminating of the artificial viscosity and accounting of the physical viscosity; it allows to obtain the stable numerical solution by using of a fine enough computational grid [26]. Eq. (7) for the dislocation velocity is solved with use of the approximate analytical solution [15]. All other equations are solved by Euler method with a varied time step.

## 5 CALCULATION RESULTS

In this section we present some results obtained with use of the described above plasticity model with the kinetics of structural defects.

### 5.1 Strain rate dependence of the dynamic yield strength

Fig. 1 presents our calculated strain rate dependences of maximum shear stress in the coarse grained copper (the limit $d \to \infty$) with varied initial dislocation densities in comparison with the experimental and calculated data taken in its adapted form from [27]. A uniaxial compression of a small substance volume had been simulated with the constant strain rate $\partial v / \partial z = \dot{\varepsilon}$ to obtain each point of these dependences.

The presented in Fig. 1 maximal shear stress is equal to the one half of the dynamical yield strength. The experimental and calculated dependences have two distinct regions: at the low and moderate strain rates the dynamic yield strength increases slowly with the strain rate–the regime of dislocation velocity control according to [27], while after some point the shear stress growth becomes very sharp–the regime of dislocation generation control [27]. This sharp growth of shear strength is a manifestation of the dislocation starvation, and the used dislocation plasticity model can uniformly describe both regimes. According to our modeling, the different strain rate dependences ascertained in [27] can be explained by different initial densities of structural defects (dislocations) in the loaded material. Increase of initial defects concentration leads to decrease of the shear strength at high strain rates $>10^6$ $s^{-1}$.

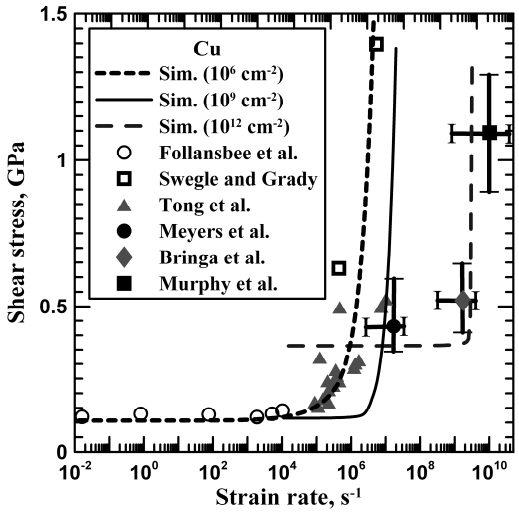


**Figure 1**: Strain rate dependences of maximal shear stress (the dynamical yield strength) for coarse-grained copper. Markers are experimental and calculated (MD) results of different authors taken from [27]. Lines present our simulation results for various initial dislocation densities. Scattering of experimental points at large strain rates can be explained by difference of the initial dislocation density of samples.

### 5.2 Localization of plastic flow on the shock front

The proposed model has been used for numerical investigation of the plastic flow localization [28]. Fig. 2 shows the picture of the plastic flow localization behind the shock wave front. The shock wave moves through a sample with the randomly perturbed dislocation density. One can see formation of the shear bands inclined on 45 degrees to the shock wave front. The similar results have been obtained for perturbation of grain size; any investigated perturbation leads to nonuniformity.

## 6 CONCLUSIONS

- Following the dynamics and kinetics of structural defects is a natural way to accounting of inertness of the plastic relaxation. This approach can be used for construction of a wide-range plasticity model as an important element of the constitutive equations for the continuum mechanics modelling.
- Here we present the plasticity model which takes simultaneously into account the dislocations gliding, the twinning and the grain boundary sliding as competing plasticity mechanisms. This approach gives results corresponding to the experimental data. It can be extended further by accounting of additional physical processes.
- The proposed approach allows to calculate the modification of defects subsystems and the correlated mechanical properties during the dynamic loading.
- At the high strain rates $>10^6\ s^{-1}$ the inertness of plasticity plays the critical role: the shear strength depends very much on the initial concentration of defects. Increase of the initial dislocation density leads to the decrease of the shear strength at such conditions.

This work is supported by grant of the President of Russian Federation (MD-286.2014.1) and by the Russian Foundation for Basic Research (Grant Nos. 12-02-31375, 14-01-31454).

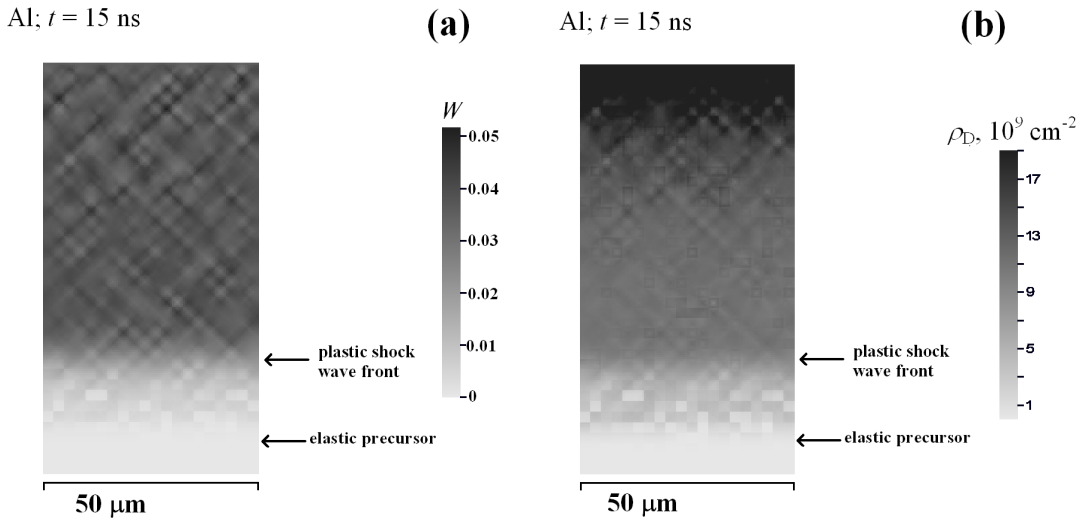


**Figure 2**: Localization of plastic flow on the shock wave front: the shock wave propagation in aluminium with the randomly perturbed initial distribution of dislocation density; the plastic strain intensity (a) and the dislocation density (b). Formation of shear bands inclined on 45 degrees to the shock wave front. Velocity jump in the shock wave is 0.3 km/s, it moves downwards.

## REFERENCES


[1] Whitley, V.H., McGrane, S.D., Eakins, D.E., et al. The elastic-plastic response of aluminum films to ultrafast laser-generated shocks. *J. Appl. Phys.* (2011) **109**:013505.

[2] Inogamov, N.A., Zhakhovsky, V.V., Petrov, Yu.V. et al. Electron-Ion Relaxation, Phase Transitions, and Surface Nano-Structuring Produced by Ultrashort Laser Pulses in Metals. *Contrib. Plasma Phys.* (2013) **53**:796-810.

[3] Krasnikov, V.S., Mayer, A.E. and Yalovets, A.P. Dislocation based high-rate plasticity model and its application to plate-impact and ultra short electron irradiation simulations. *Int. J. Plast.* (2011) **27**:1294-1308.

[4] Mayer, A.E., Khishchenko, K.V., Levashov, P.R. and Mayer, P.N. Modeling of plasticity and fracture of metals at shock loading. *J. Appl. Phys.* (2013) **113**:193508.

[5] Borodin, E.N., Atroshenko S.A. and Mayer, A.E. Distribution of dislocations and twins in copper and steel samples after shock loading. *Techn. Phys.* (2014) – in press.

[6] Borodin, E.N. and Mayer, A.E. A simple mechanical model for grain boundary sliding in nanocrystalline metals. *Mater. Sci. Eng. A.* (2012) **532**:245-248.

[7] Borodin, E.N. and Mayer, A.E. Yield strength of nanocrystalline materials under high-rate plastic deformation. *Phys. Solid State* (2012) **54**:808-815.

[8] Krasnikov, V.S. and Mayer, A.E. Numerical investigation of the change of dislocation density and microhardness in surface layer of iron targets under the high power ion- and electron-beam treatment. *Surf. Coat. Techn.* (2012) **212**:79-87.

[9] Kolgatin, S.N. and Khachatur'yants, A.V. Interpolation equations of state of metals. *Teplofiz. Vys. Temp.* (1982) **20**:90-94.

[10] Fortov, V.E., Khishchenko, K.V., Levashov, P.R. and Lomonosov, I.V. Wide-range multi-phase equations of state for metals. *Nucl. Instrum. Meth. Phys. Res. A* (1998) **415**:604-608.

[11] Landau, L.D. and Lifshitz, E.M. *Course of Theoretical Physics*. Pergamon, New York, Vol. VII (1986).
[12] Guinan, M.W. and Steinberg, D.J. Pressure and temperature derivatives of the isotropic polycrystalline shear modulus for 65 elements. *J. Phys. Chem. Solids* (1974) **35**:1501-1512.
[13] Wilkins, M.L. Calculation of elastic-plastic flow. UCRL-7322 (1963).
[14] Kosevich, A.M. Dynamical Theory of Dislocations. *Sov. Phys. Uspekhi* (1965)**7**:837-854.
[15] Dudorov, A.E. and Mayer, A.E. Equations of dislocation dynamics and kinetics at high rates of plastic deformation. *Vestn. Chelyab. State Univ. Phys.* (2011) **39**:48-56.
[16] Al'shitz, V.A. and Indenbom, V.L. Dynamic dragging of dislocations. *Sov. Phys. Uspekhi* (1975) **18**:1-20.
[17] Suzuki, T., Takeuchi, S. and Yoshinaga, H. *Dislocation Dynamics and Plasticity*. Springer, Berlin (1991).
[18] Allain, S., Chateau, J.-P. and Bouaziz O. A physical model of twinning-induced plasticity effect in a high manganese austenitic steel. *Mater. Sci. Eng. A* (2004) **387-389**:143-147.
[19] Christian, J.W. and Mahajan, S. Deformation twinning. *Prog. Mat. Sci.* (1995) **39**:1-157.
[20] Eshelby, J.D. The determination of the elastic field of an ellipsoidal inclusion and related problems. *Collected works of J.D. Eshelby.*
[21] Kittel, C. *Introduction to Solid State Physics.* Wiley, New York, (2004).
[22] Plekhov, O.A., Naimark, O.B., Saintier, N., Palin-Luc, T. Elastic–plastic transition in iron: structural and thermodynamic features. *Tech. Phys.* (2009) **54**:1141–1146.
[23] Swygenhoven, H.V. and Caro, A. Plastic behavior of nanophase metals studied by molecular dynamics. *Phys. Rev. B* (1998) **58**:11246–11251.
[24] Chuvildeev, V.N. *Nonequilibrium Grain Boundaries in Metals: Theory and Application*. Fizmatlit, Moscow, (2004).
[25] Yalovets, A.P. Calculation of flows of a medium induced by high-power beams of charged particles. *J. Appl. Mech. Tech. Phys.* (1997) **38**:137–150.
[26] Mayer, A.E. and Khishchenko, K.V. Numerical study of shock-wave structure in elastic-plastic medium. *Physics of Extreme States of Matter–2014*. JIHT RAS, Moscow, (2014):45-48.
[27] Armstrong, R.W. and Zerilli, F.J. High rate straining of tantalum and copper. *J. Phys. D: Appl. Phys.* (2010) **43**:492002.
[28] Mayer, A.E., Borodin, E.N. and Mayer, P.N. Localization of plastic flow at high-rate simple shear. *Int. J. Plast.* (2013) **51**:188-199.